Journal of
Composites Science

MDPI

Article

An Investigation of the Thermal Properties of LM13- Quartz-Fly-Ash Hybrid Composites

B. R. N. Murthy, Amar Murthy Ambekar * and Anupama Hiremath

Manipal Institute of Technology, Manipal Academy of Higher Education, Manipal 576104, Karnataka, India; murthy.brn@manipal.edu (B.R.N.M.); anupama.hiremath@manipal.edu (A.H.)
* Correspondence: amar.murthy@manipal.edu

Abstract: In the present work, a metal–matrix composite was casted using the LM13 aluminum alloy, which is most widely used for casting automotive components. Such applications require materials to withstand high operating temperatures and perform reliably without compromising their properties. In this regard, particulate-reinforced composites have gained widespread adaptability. The particulate reinforcements used comprise of one of the widely available industrial by-products. which is fly ash, along with the abundantly available quartz. Hybrid composites are fabricated through the economical liquid route that is widely used in mass production. Though there are numerous published research articles investigating the mechanical properties of metal–matrix composites, very few investigated the thermal properties of the composites. In the present work, thermal properties such as thermal conductivity and thermal diffusivity of cast hybrid composites were evaluated. The particulate reinforcements were added in varied weight percentages to the molten LM13 alloy and were dispersed uniformly using a power-driven stirrer. The melt with the dispersed particulate reinforcements was then poured into a thoroughly dried sand mold, and the melt was allowed to solidify. The quality of the castings was ascertained through density evaluation followed by a microstructural examination. It was found that the composites with only the fly ash particles as a reinforcement were less dense in comparison to the composites cast with the quartz particulate reinforcement. However, the hybrid composite, with both particulate reinforcements were dense. The microstructure revealed a refined grain structure. The thermal diffusivity and thermal conductivity values were lower for the composites cast with only the fly ash reinforcement. On the other hand, the composites cast with only quartz as the particulate reinforcement exhibited higher thermal diffusivity and thermal conductivity. The specific heat capacity was found to be lower for the fly ash-reinforced composites and higher for the quartz-reinforced composites in comparison to the LM13 base matrix alloy. However, the highest value of thermal diffusivity and thermal conductivity were reported for the hybrid composites with a 10 wt.% inclusion of both fly ash and quartz particulate reinforcements.

Keywords: aluminum matrix composites; thermal conductivity; thermal diffusivity

Citation: Murthy, B.R.N.; Ambekar, A.M.; Hiremath, A. An Investigation of the Thermal Properties of LM13-Quartz- Fly-Ash Hybrid Composites. *J. Compos. Sci.* **2024**, *8*, 90. https://doi.org/10.3390/jcs8030090

Academic Editor: Francesco Tornabene

Received: 18 December 2023
Revised: 20 February 2024
Accepted: 21 February 2024
Published: 1 March 2024

1. Introduction

The advent of composites has widened the scope of materials with properties that can be tuned to meet specific structural and/or design requirements. Metal–matrix composites (MMCs) have illustrated properties and performances that are superior to those of their conventional, monolithic metallic counterparts [1]. Advancements in research on MMCs have resulted in overcoming challenges such as economical processing, design and characterization of composite materials along with an improved understanding of the interfacial interactions between the matrix and the selected reinforcements [2]. Also, the study of MMCs is constantly broadening due to the fact that such materials can be fabricated through the incorporation of a huge mix of reinforcements that are added to the matrix with the possibility of varying not only their type, but also their size, shape and content [3]. Further, it was observed that such variations tend to tune the final composite properties and

provide the designer with innumerable options to come up with a material which suits the targeted application [4–6]. Amongst the innumerable types of reinforcement, ceramic reinforcements, in both micro and nano scales, have attracted the highest interest [7]. MMCs, due to the merging of the properties of the base alloy and the ceramic reinforcements, possess a superior combination of properties such as ductility coupled with improved toughness and reduced weight with high strength [8]. Owing to such advantages, MMCs have become candidate materials for applications in the defense, automobile, aerospace, electronics, electrical, marine and infrastructure sectors [9]. Of late, industries and academic research have concentrated their attention on hybrid composites which incorporate more than one type of reinforcement within the matrix to infuse the soft, ductile matrix alloy with strength and stiffness derived from the hard, brittle reinforcements [10,11].

Amongst various MMCs developed for both research and industrial applications, aluminum and its alloys are extensively used as matrix materials. The reason for such selection is because aluminum is a light metal, and lightness is the primary requirement for most of the commercial MMCs that are in use today. Another contributing factor is that amongst the other available light metals such as titanium and magnesium, aluminum is comparatively inexpensive and is available in abundance. Aluminum–matrix composites (AMCs) have been used extensively in the aerospace and automotive sectors as they provide a good strength-to-weight ratio [12,13], a primary requirement to reduce fuel costs. Also AMCs exhibit improved resistance to corrosion and deformation, combined with excellent strength and elastic modulus [14,15]. AMCs reinforced with particles derived from oxides and carbides of ceramic materials such as SiC, Al_2O_3, B_4C, SiO_2, WC and MgO possess superior mechanical, thermal and electrical properties and were shown to perform better than their monolithic metallic counterparts in severe operating conditions requiring resistance to high temperatures and pressures [16–19]. Karthikraja et al. reported that the inclusion of SiC and Al_2O_3 particles within an aluminum alloy (Al 7075) matrix resulted in the production of stronger interfaces between the particles and the matrix alloy, which in turn reduced the rate of corrosion [20]. Similar findings were published by Ferraris et al., who concluded that SiC_p as a reinforcement in an aluminum matrix results in improved resistance to corrosion and hence can be used in braking applications [21]. Xu et al. experimentally compared the effect of the addition of micro and nano B_4C particles on the morphology and mechanical properties of AMCs. They concluded that both micro and nano B_4C particles had good wettability in the aluminum matrix and the morphology of the AMCs improved with the improvement in their mechanical properties [22]. Messer et al. reported that improvement in the mechanical properties of AMCs can be obtained through the addition of coarse particles rather than fine particles [23].

To make AMCs viable for large-scale commercial production, it is imperative to reduce the cost of such materials through the selection of proper processing techniques and reinforcements. Researchers are trying to obtain AMCs reinforced with cheaper and easily available materials which include industrial wastes and by-products; this would not only decrease the cost of the final material but also ensure effective waste management [24–26]. Quartz (SiO_2) is a natural mineral that is hard and crystalline in form. Due to its ceramic nature and wide availability, it is used as a reinforcement in various MMCs. Malaki et al. reported that the inclusion of nano SiO_2 particles improved AMCs' tensile and compressive strength [27]. Tirfe et al. prepared Al6061/Al_2O_3/quartz hybrid AMCs and concluded that the hardness, compressive and impact strength of the AMCs improved with the addition of the optimum content of quartz particles [28]. Fly ash, a type of industrial waste, is yet another promising reinforcing material that has found increased usage to reinforce AMCs in recent years. Matti et al. reported the improvement in tribological characteristics of Al7075/red mud/fly ash/mica hybrid AMCs [29]. Soundararajan et al. confirmed that the improved wear resistance of A356/fly ash AMCs was due to increased bonding of the fly ash particles with the A356 aluminum alloy [30]. Reddy et al. highlighted that through the addition of fly ash to Al_2O_3-reinforced AMCs, there was a reduction in the weight as well as in the cost of the AMCs [31].

The selection of a proper processing methodology is also essential to ensure the success of AMCs. The fabrication route selected should be cost-effective and should ensure a uniform distribution of the selected particles within the matrix. Liquid state processing such as melt stir casting is considered to be an effective method to fabricate particulate-reinforced AMCs [32,33]. Stir casting is one such processing route which has universal commercial acceptability to fabricate AMCs owing to its flexibility, ability to cast intricate geometries and cost-effectiveness [34,35]. The selection of casting as the processing method invariably calls for setting up a rapid abstraction of heat from the melt to ensure directional solidification resulting in a refined grain structure and quality castings [36,37]. End chills are used to promote the directional solidification of the casting, thus enabling the production of defect-free AMCs [38,39]. Sunil Kumar et al. studied the effect of copper end-chill on the fatigue characteristics of A356/hematite AMCs. They reported that AMCs cast with copper end-chill possessed a significantly improved fatigue strength in comparison to AMCs cast without the use of the copper chill [40]. Vijay Kumar et al. studied the effect of different end chills on the mechanical properties of Al356/ZrO_2/SiC hybrid AMCs and found that AMCs cast with copper end-chill had superior mechanical properties [41]. Ravitej et al. casted LM13/zircon/carbon AMCs using copper end-chill to induce directional solidification and concluded that such AMCs had improved wear resistance over AMCs cast using without end chill [42].

Most of the published works in the field of hybrid AMCs discuss the mechanical and tribological properties of the composites, and there is a serious dearth of scientific reports that highlight the thermal properties of hybrid AMCs. The investigation of the thermal properties of AMCs is of prime importance due to the fact that these composites are highly recommended for automotive applications wherein materials are subjected to high operating temperatures. At such high temperatures, materials should perform reliably without deterioration of their physical and mechanical properties. The present paper discusses the effect of the addition of quartz and fly ash as particulate reinforcements in varied weight percentages to an LM13 aluminum alloy matrix to cast hybrid AMCs via the stir casting method through the employment of a metallic end-chill made of copper. Further, an effort was made to study the coefficients of thermal expansion and thermal conductivity of the cast hybrid composites to analyze the effect of variations in the reinforcement content and the chilling effect on the thermal properties of the cast hybrid composites.

2. Materials and Methods

2.1. Matrix Material

The LM13 aluminum alloy was used as the matrix material. Table 1 illustrates the elemental composition of the LM13 alloy. The LM13 alloy is extensively used for automotive applications owing to its excellent fluidity [43,44] that enables the production of large castings and good thermal resistance with a low coefficient of thermal expansion [45,46] that ensures dimensional stability of the castings under high-temperature applications along with good strength to sustain the applied loads. An additional feature that supports the use of LM13 in the production of automobile parts is the ease of machinability [47] that is rendered by the presence of a high quantity of silicon.

Table 1. Elemental composition of LM13.

Elements	Weight Percent (Approx.)
Silicon	11.00
Nickel	1.50
Magnesium	1.0
Copper	1.0
Iron	0.8
Manganese	0.5
Aluminum	Balance

2.2. Particulate Reinforcements

Quartz and fly ash with an average particle size of 25–40 μm were incorporated as particulate reinforcements to impart additional hardness and strength to the otherwise soft and ductile matrix material. Quartz has the ability to maintain dimensional stability even at very high temperatures due to the silicon particles present in it. Composites, to be sustainable and economically viable, should be composed of industrial by-products. Fly ash is produced in large quantities as a by-product in industries that burn coal for the generation of heat. Fly ash can be a good reinforcement in metallic matrices due to its low density that allows for its uniform dispersion within the matrix material; at the same time, it is widely available at low prices. Table 2 provides the chemical composition of fly ash.

Table 2. Chemical composition of fly ash.

Chemical Compounds	Weight Percent (Approx.)
Silicon dioxide	55
Aluminum oxide	26
Iron oxide	7
Calcium oxide	9
Magnesium oxide	2
Sulfur trioxide	1

2.3. Composition of the Composites

The composites in the present work were casted in a sand mold through the incorporation of the particulate reinforcements that were added to the LM13 matrix in different weight percentages. The configurations of the composites that were casted in the current work are provided in Table 3.

Table 3. Composite configurations.

Composite Coding	LM13 (M) (Wt.%)	Quartz (Q) (Wt.%)	Fly Ash (F) (Wt.%)
M1Q0F0	100	0	0
M95Q5F0	95	5	0
M90Q10F0	90	10	0
M95Q0F5	95	0	5
M90Q0F10	90	0	10
M90Q5F5	90	5	5
M80Q10F10	80	10	10

2.4. Composite Fabrication

The stir casting method was used to melt the matrix alloy and evenly disperse the particulates within the melt. LM13 ingots were melted at around 750 °C in an electric furnace. Preheating of the quartz and fly ash particulates was performed, and the reinforcements were heated to about 300 °C. Preheating ensures that the reinforcements are free from any volatile particles and moisture. The required quantities of preheated particulates were weighed and added to the molten matrix alloy. In order to evenly disperse the particulates within the molten matrix material and keep them suspended in the melt, the melt along with the particulates was agitated using a power-driven agitator at a speed of 800 rpm for a duration of 300 s. Figure 1 illustrates the experimental setup used to melt and disperse the particulates within the matrix material. The well-agitated molten LM13 with the added reinforcements was further introduced into dry sand molds to produce rectangular castings of 150 × 20 × 25 mm dimensions.

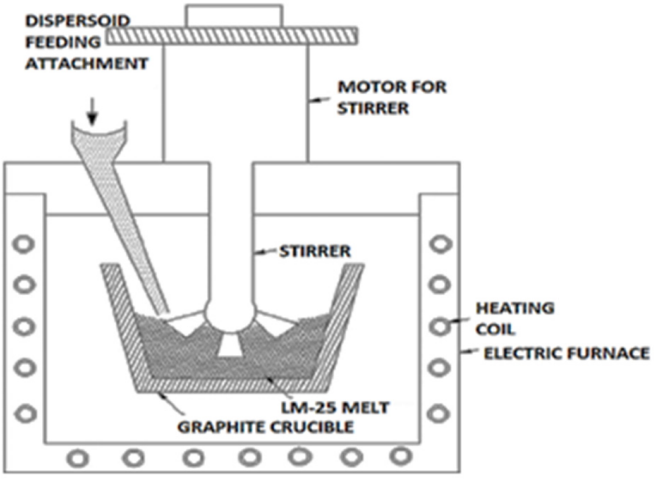

Figure 1. Stir casting setup.

Figure 2 shows the sand mold prepared to cast the required composites along with the provision to insert the chill. The specimens required for the thermal property tests were drawn from the cast composite from the end that was near the chill application area.. Rectangular specimens measuring 10 × 5 × 5 mm were machined from the cast composite near the chill application area on the milling machine using an end mill. The machined specimens were then polished using emery paper. Figure 3 illustrates the specimen set in wax molds for microstructural examination.

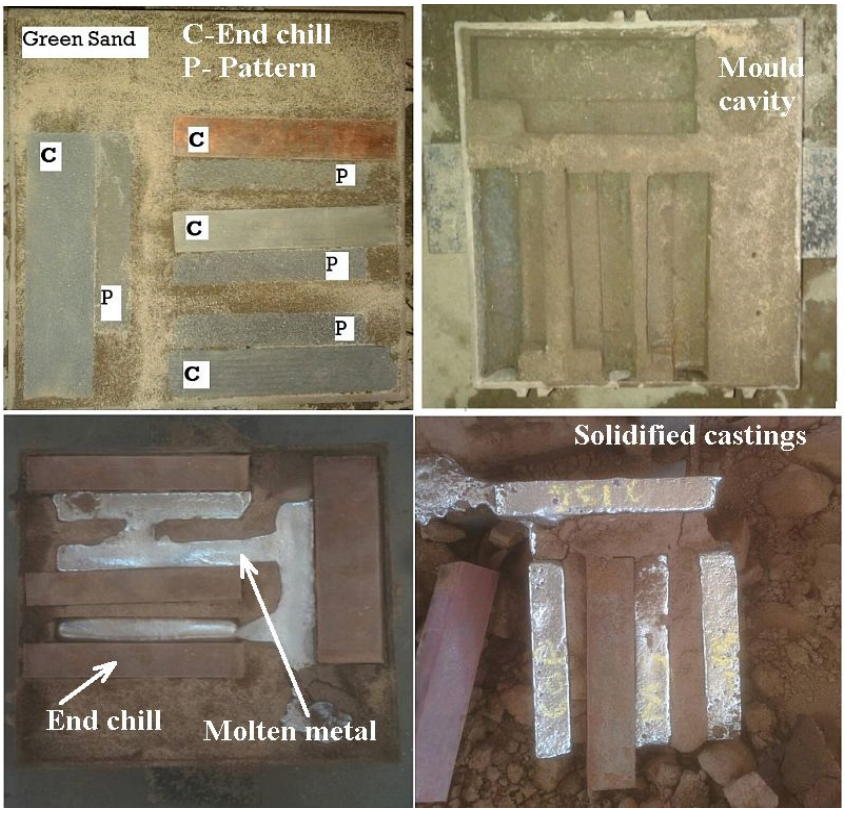

Figure 2. Sand mold with patterns inserted for casting and end chills.

Figure 3. Specimen set in wax molds for microstructural examination.

2.5. Evaluation of the Density and Porosity of the Composites

The theoretical density of the cast composites was determined through the Agarwal and Broutman Equation (1) [48]. Here, the density is indicated by 'ρ', the weight fraction is represented by 'W', 'M' represents the LM13 matrix material, 'Q' stands for quartz, and 'F' denotes the fly ash particulates. The density values, expressed as g/cc, for LM13, quartz and fly ash were 2.81, 2.2 and 1.9, respectively. The experimental density of the cast composites was determined through the simple Archimedean water displacement method conducted in ambient conditions [49].

$$\rho_{theoretical} = \frac{1}{\left(\frac{W_F}{\rho_F}\right) + \left(\frac{W_Q}{\rho_Q}\right) + \left(\frac{W_M}{\rho_M}\right)} \quad (1)$$

The porosity of the cast AMCs was determined using Equation (2) [50]

$$Porosity\ \% = \frac{\rho_{theoretical} - \rho_{experimental}}{\rho_{theoretical}} \times 100 \quad (2)$$

2.6. Thermal Property Evaluation Procedure

The laser flash method was employed for evaluating the thermal conductance of the cast composites. Thermal diffusivity was determined through the aid of the NETZCH NanoFlash device. The thermal conductivity of the cast composite specimens was calculated with the aid of the obtained diffusivity values. The test was performed in adherence to standard testing principles as per ASTM E-1461. The apparatus was equipped with a furnace that could be operated at a temperature between room temperature and 300 °C. Computerized data acquisition was accomplished by integrating the apparatus with a 32-bit computer with the Windows operating system in which Proteus® software (version 8.17) was installed. In the laser flash technique, the front side of the sample is heated with the help of a light pulse. As the heat transfers through the bulk of the composite specimen, the rear side of the specimen experiences an increment in its surface temperature. This rise in temperature is recorded by an infra-red detector. The resulting temperature-against-time curve is analyzed to obtain the thermal diffusivity of the sample. The computation of the product of the composite's density, specific heat capacity and thermal diffusivity yields the thermal conductivity (λ) of the composite. To determine the heat capacity per unit mass, a heat flux differential scanning calorimeter (DSC) was employed. The DSC was

operated over a temperature range from 20 °C to 300 °C at a heating rate of 10 °C/min. The composite's thermal conductivity was computed as shown in Equation (3)

$$\lambda(T) = \alpha(T) \times cp(T) \times \rho(T) \quad (3)$$

Here, the terms λ(T), α(T) and cp(T) stand for thermal conductivity, thermal diffusivity and specific heat capacity, respectively. The specimens were subjected to heating from a laser flash source until their temperature rose from room temperature to 300 °C. The specimens were smeared with a thin layer of graphite to aid the absorbance and emittance of the flash from its front and rear side, respectively. An infra-red detector detected and recorded the temperature increment ensuing at the rear end of the composites. Thermal diffusivity was calculated by the machine's software using the relation provided in Equation (4).

$$\alpha = 0.1388\left(\frac{d^2}{t_{1/2}}\right) \quad (4)$$

In Equation (3), 'α' is thermal diffusivity, 'd' is the thickness of the specimen, and '$t_{1/2}$' is time at 50% of the temperature increase.

3. Results and Discussions

3.1. Density of the Composites

Figure 4 depicts the theoretical and experimental densities of the cast composites. The analysis of the obtained results indicated that dense castings were formed. This was indicated by the experimental values of the density that deviated slightly from the theoretical density values. Figure 5 shows the porosity percentage for the cast AMCs. The porosity of the AMCs was higher with the inclusion of fly ash particles in comparison to the inclusion of quartz particles. However, the porosity of all the cast AMCs did not exceed 4%, which is, as per the available literature, an acceptable level [51]. The results also indicated that the selected method of processing was well suited to produce dense castings. This fact was further supported by the microstructural analysis. Figure 6 shows the microstructure of the cast composites. The microstructure of the composite specimens, observed using an optical microscope, was characterized by the presence of eutectic silicon within inter-dendritic regions. Also observed were fine precipitates of the elements that formed the LM13 alloy. This showed that there was a closer arrangement of grains with high refinement in their structure. Particulates usually become entrapped within dendrites during the solidification process and are pushed at their end, forming a tip at their base. Such particle entrapment can be seen in Figure 6e. Shrinkage porosity is more pronounced in Figure 6b,c pertaining to AMCs cast with fly ash reinforcements. For the hybrid AMCs, the microstructure was characterized by fine shorter Si needles and a nearly globular Al-Si eutectic phase. This indicated that hybridization through the addition of quartz and fly ash particles was beneficial for the quality of the AMCs produced.

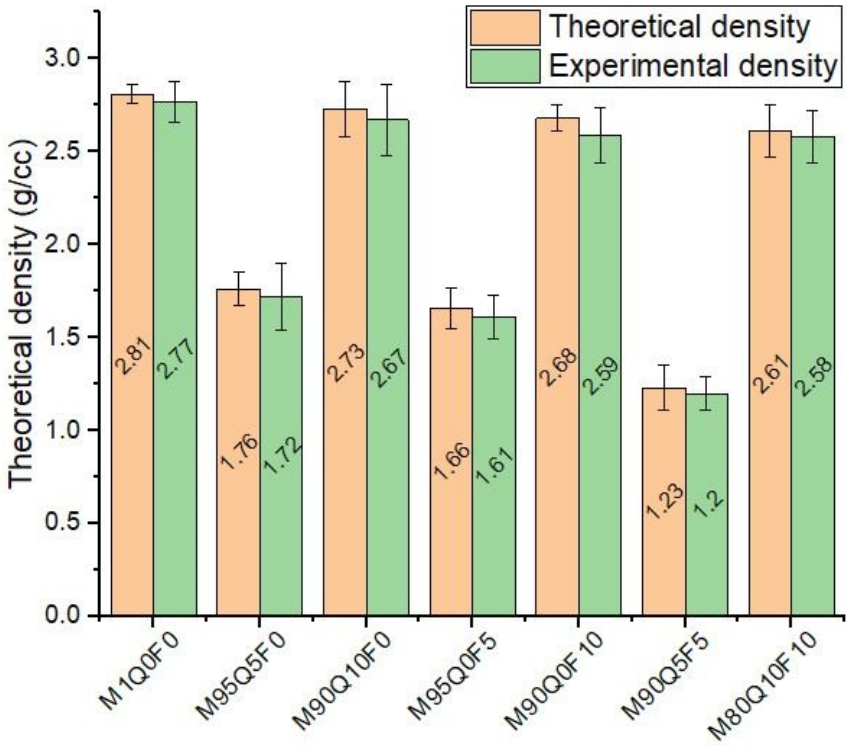

Figure 4. Theoretical and experimental densities of the cast composites.

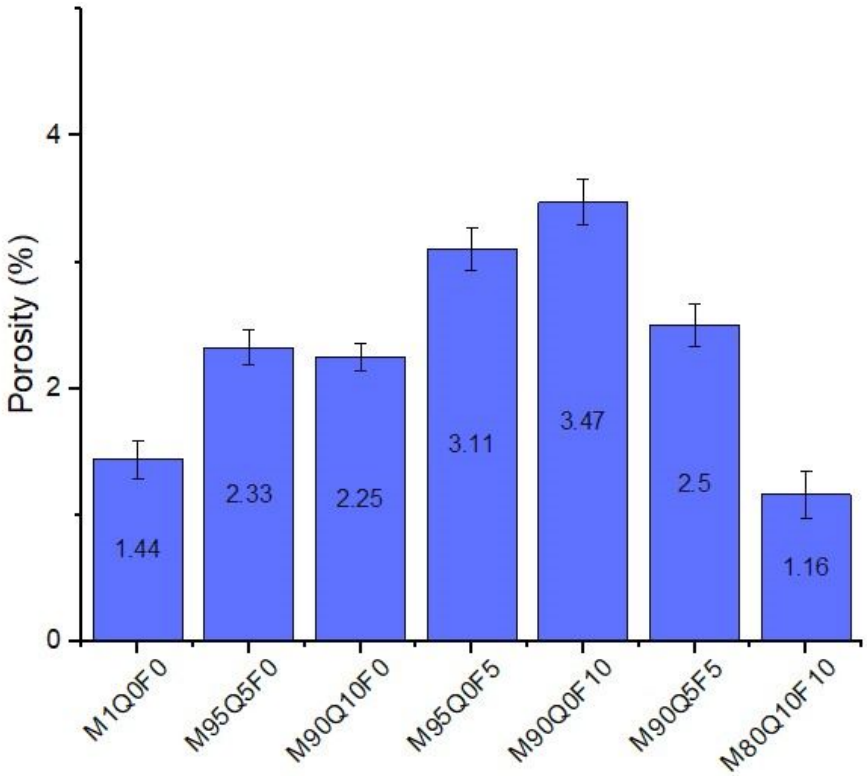

Figure 5. Porosity of the cast composites.

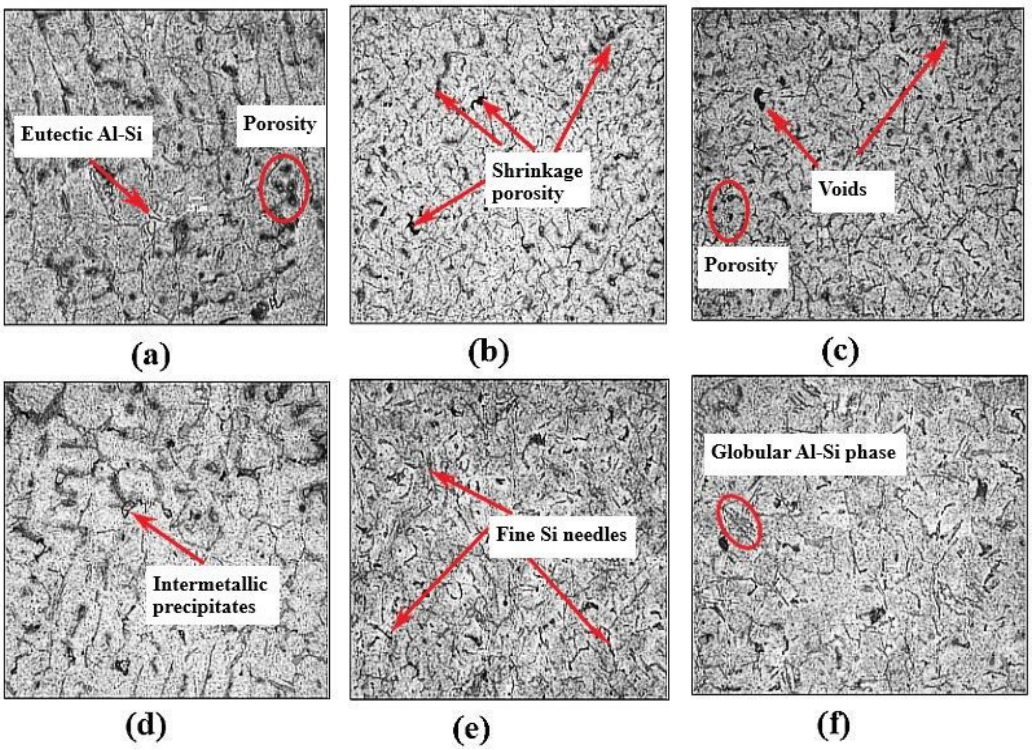

Figure 6. Microstructure of the cast composites. (**a**) M1Q0F0, (**b**) M95Q0F5, (**c**) M90Q0F10, (**d**) M90Q10F0, (**e**) M90Q5F5, (**f**) M80Q10F10.

3.2. Thermal Diffusivity of the Composites

Figure 7 depicts the variation of thermal diffusivity and thermal conductivity of the cast hybrid composites with temperature.

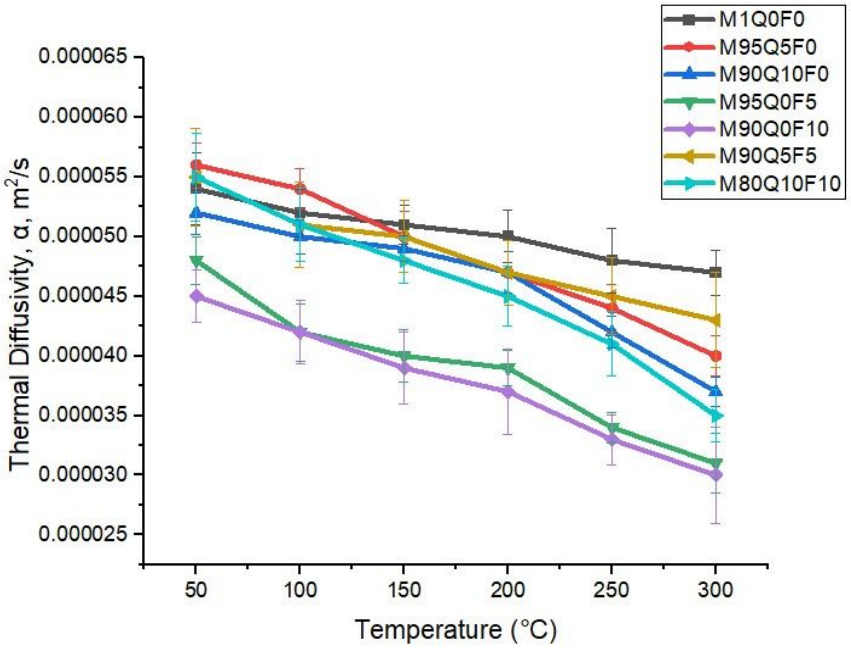

Figure 7. Thermal diffusivity of the cast composites.

Thermal diffusivity provides an indication of the capability of a material to dissipate heat with respect to time. The materials employed in applications requiring a fast dissipation of heat should possess a high thermal diffusivity. The analysis of the results indicated that amongst the cast composites, the thermal diffusivity of the M95Q0F5 and M90Q0F10

AMCs with only fly ash as a reinforcement was very low compared to that of the AMCs cast with only quartz as a reinforcement. Also, the M90Q0F10 AMCs showed the lowest thermal diffusivity in comparison to all other cast AMCs. This could be due to the physical characteristics of the fly ash particles, which tend to be irregularly shaped, with hollow spherical particulates scattered within the mass of fly ash [52]. The hollow particles are usually filled with air or any low-thermal-conductivity gas [53]. The presence of a gaseous phase within the hollow fly ash particles hinders the easy dissipation of heat. However, for the M95Q5F0 and M90Q10F0 AMCs with only quartz as a reinforcement, we observed that the thermal diffusivity was higher in comparison to that of the composites with only fly ash as a reinforcement. This may be attributed to the physical characteristics of quartz, which is a solid crystal, unlike hollow fly ash. For the hybrid AMCs, thermal diffusivity was high for M90Q5F5 in comparison to M80Q10F10. Thus, it was inferred that the fly ash reinforcement did not allow for an easy dissipation of heat through the AMCs, whereas on the other hand, the quartz particulate reinforcement helped to accelerate the heat dissipation through the bulk of the AMCs.

3.3. Specific Heat Capacity of the Composites

Specific heat capacity denotes the amount of energy/heat required to raise the temperature of AMCs of a given mass by 1 °C. Figure 8 shows the specific heat capacity of the cast AMCs. It can be seen that the addition of quartz particles reduced the specific heat capacity of the AMCs. The morphology of the AMCs aid in understanding the variation in heat capacity of the materials. It is generally understood that pores and/or voids act as heat reservoirs due to the entrapment of air within them. Hard quartz particles act as strong mechanical reinforcements, reducing matrix shrinkage during the solidification process [54]. This helps in controlling the porosity of AMCs, and thus the specific heat capacity of such AMCs decreases. The specific heat capacity of the 5 wt.% particle-reinforced M95Q5F0 AMCs was reduced by 8% when quartz, rather than fly ash, was used as a reinforcement. Similarly, the specific heat capacity of the 10 wt.% particle-reinforced M90Q10F0 AMCs was reduced by 10% when quartz, rather than fly ash was used as a reinforcement. The addition of fly ash, however, increased the specific heat capacity of the AMCs, which was found to be greater than that of the unreinforced LM13 alloy. This could be associated with the generation of voids and/or air pockets within the fly ash-reinforced AMCs. Due to such voids, the density of the M90Q5F5 and M80Q10F10 AMCs with only fly ash as a reinforcement was lower in comparison to that of the M95Q5F0 and M90Q10F0 AMCs which were cast through the inclusion of only quartz particles as a reinforcement. The density of the M95Q0F5 AMC was approximately 42% lower than that of the LM13 alloy (M1Q0F0 AMC), while the density of the M90Q0F10 AMC was nearly 7% lower than that of the unreinforced M1Q0F0 AMC. On the other hand, the density of the M95Q5F0 and M90Q10F0 AMCs was approximately 38% and 4% lower than that of the M1Q0F0 AMC, respectively. Air, which is a heterogenous mixture of several gases, has a specific heat capacity of 1000 J/kgK at constant pressure, which is high in comparison to the specific heat capacity of LM13, which is 872 J/kgK. The inclusion of air within AMCs tend to increase the heat storage capacity of AMCs. Thus, fly ash-reinforced AMCs are suitable to be employed in such applications wherein the required material needs to act as a thermal reservoir.

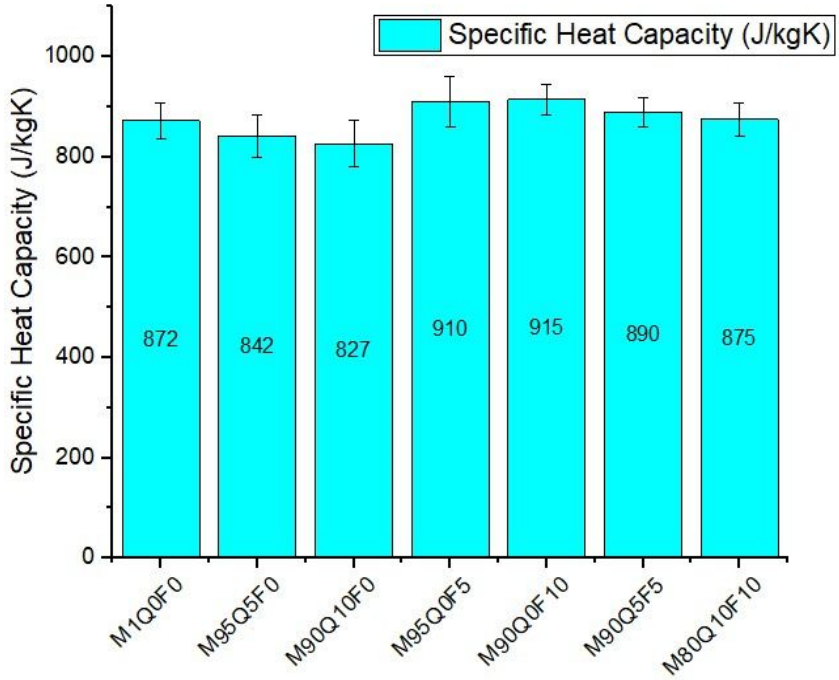

Figure 8. Specific heat capacity of the cast composites.

3.4. Thermal Conductivity of the Composites

Thermal conductivity is the ability of a material to conduct heat with respect to time. A high thermal conductivity is desirable in applications such as electronic packaging and automotive component manufacturing, where it is required to transfer heat quickly to a cooling medium. Figure 9 shows the variation of thermal conductivity of the cast AMCs depending on the type and wt.% inclusion of the particulate reinforcements.

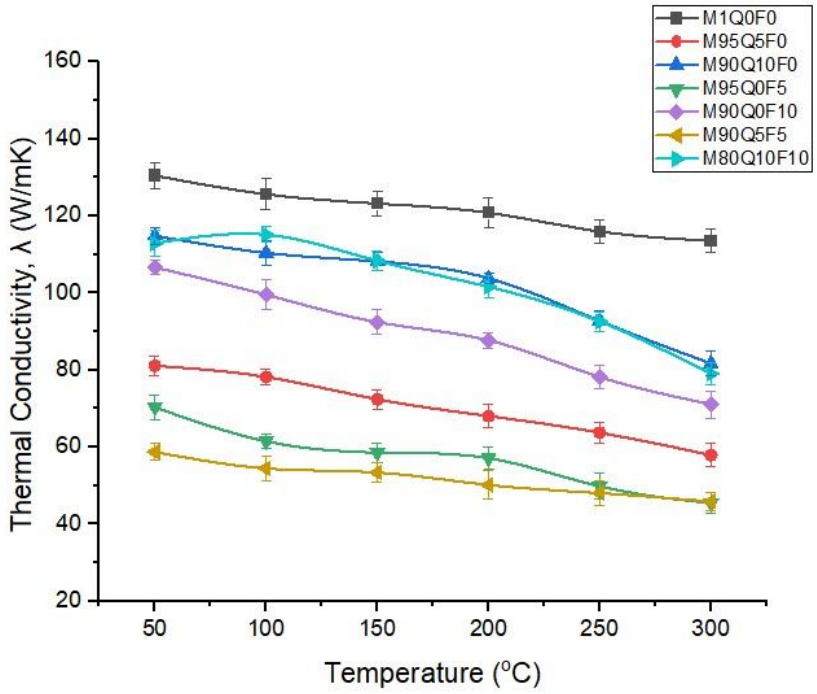

Figure 9. Thermal conductivity of the cast composites.

The obtained results indicated that the composites with quartz as a reinforcement had higher thermal conductivity in comparison to the composites cast with the addition

of only the fly ash particulate reinforcement. The thermal conductivity of the M95Q5F0 and M90Q0F0 AMCs was found to be 63.72 and 92.74 W/mK, respectively, at 250 °C. On the other hand, the M95Q0F5 and M90Q0F10 AMCs possessed a thermal conductivity of 49.81 and 78.20 W/mK, respectively, at 250 °C. The thermal conductivity at 250 °C of the 5 wt.% fly ash-reinforced M95Q0F5 AMC was approximately 21.82% lower than the thermal conductivity of the 5 wt.% quartz-reinforced AMC at the same temperature. This could be due to structural properties of fly ash, which is a porous material [55,56]. Any entrapment of air and gas cannot be ruled out in such porous structures. Air has a very low thermal conductivity and creates a barrier for the flow of heat through the material, which reduces the overall thermal conductivity of the material. Quartz, on the other hand, is an irregularly shaped ceramic material which is characterized by a high thermal conductivity [57]. The M90Q10F0 composites cast with only quartz as a reinforcement tended to have a higher thermal conductivity in comparison to the other composites cast in this study. The irregularly shaped quartz particles have many active surfaces that promote a stronger adhesion with a matrix material than the smooth fly ash particles. This makes AMCs denser with fewer pores. For the hybrid composites, thermal conductivity was high for the M80Q10F10 AMCs and low for the M90Q5F5 AMCs. At 250 °C, the thermal conductivity of the M80Q10F10 AMCs was 92% higher than the thermal conductivity of the M90Q5F5 AMCs. Of all the cast AMCs, M90Q5F5 had the lowest thermal conductivity of 48.06 W/mK, while the M80Q10F10 AMC had the highest thermal conductivity of 92.55 W/mK. This indicated that a 5 wt.% inclusion of quartz was not sufficient to make the AMC denser with reduced porosity and, thus, that the effect of 5 wt.% fly ash was more pronounced in M90Q5F5 AMCs. With a 10 wt.% inclusion of both quartz and fly ash in M80Q10F10, the mechanical reinforcement of the matrix became sufficiently high, which in turn reduced the shrinkage porosity; in addition, there was good intermetallic bonding between the matrix and the reinforcing particles. Such bonding helps to improve the thermal conductivity of AMCs. Thus, it can be concluded that hybridization is an effective way to tailor and tune the thermal conductivity of composites to suit specific requirements.

4. Conclusions

The idea behind the use of composite materials in place of conventional materials is to decrease the cost and weight of materials without compromising their other properties. The incorporation of industrial waste in the form of fly ash and abundantly available resources such as quartz as reinforcements is greatly beneficial for decreasing the cost as well as the weight of materials. The composites cast with only fly ash as a reinforcement were less dense in comparison to the composites having only quartz and both quartz and fly ash as reinforcements. The density of the 5 wt.% and 10 wt.% fly ash-reinforced AMCs was reduced by nearly 42% and 7%, respectively, in comparison to that of the unreinforced AMCs, whereas the density of the 5 wt.% and 10 wt.% quartz-reinforced AMCs decreased by approximately 38% and 4%, respectively, when compared with the density of the unreinforced AMCs. The specific heat capacities of the quartz-reinforced AMCs were lower than those of the AMCs reinforced with fly ash. The thermal properties, such as thermal diffusivity and thermal conductivity, tended to be higher for the hybrid composites with both quartz and fly ash as reinforcements. Also, we can conclude that the thermal properties of the cast composites mainly depended on the characteristics of the included particulate reinforcement. The porous structure of fly ash resulted in lowering the thermal conductivity of the cast composites, while quartz, with higher thermal conductivity, was proven to be beneficial for improving the thermal conductivity of the composites. The thermal conductivity at 250 °C of the M95Q0F5 AMCs was approximately 21.82% lower than the thermal conductivity of the M95Q5F0 AMCs. Amongst all the cast AMCs, the lowest thermal conductivity of 48.06 W/mK was recorded for the M90Q5F5 AMC, and the highest thermal conductivity value of 92.55 W/mK was obtained for the M80Q10F10 AMC. Thus, through hybridization, it is possible to fine-tune the thermal properties based on the targeted application.

Author Contributions: Conceptualization and methodology, A.H.; validation, A.M.A. and B.R.N.M.; formal analysis, A.H.; investigation, A.H., A.M.A. and B.R.N.M.; resources, A.M.A.; data curation, A.H. and B.R.N.M.; writing—original draft preparation, B.R.N.M.; writing—review and editing, A.H. and A.M.A. All authors have read and agreed to the published version of the manuscript.

Funding: This research received no external funding.

Data Availability Statement: Data are available on request from the authors.

Acknowledgments: The authors would like to acknowledge the support rendered by the Advanced Composite Material Testing Laboratory during material fabrication, the Advanced Materials Testing Laboratory during testing, and the MIT Workshops in the preparation of the samples.

Conflicts of Interest: The authors declare no conflicts of interest.

References

1. Luo, K.; Xiong, H.; Zhang, Y.; Gu, H.; Li, Z.; Kong, C.; Yu, H. AA1050 Metal Matrix Composites Reinforced by High-Entropy Alloy Particles via Stir Casting and Subsequent Rolling. *J. Alloys Compd.* **2022**, *893*, 162370. [CrossRef]
2. Zhou, M.Y.; Ren, L.B.; Fan, L.L.; Zhang, Y.W.X.; Lu, T.H.; Quan, G.F.; Gupta, M. Progress in Research on Hybrid Metal Matrix Composites. *J. Alloys Compd.* **2020**, *838*, 155274. [CrossRef]
3. Zhu, Y.; Li, N.; Zhang, L.; Zhang, J.; Niu, L.; Li, W.; Li, S. Atomistic Investigation of the Effects of Different Reinforcements on Al Matrix Composite. *Metals* **2022**, *12*, 1252. [CrossRef]
4. Wu, B.; Ibrahim, M.Z.; Raja, S.; Yusof, F.; Muhamad, M.R.B.; Huang, R.; Zhang, Y.; Badruddin, I.A.; Hussien, M.; Kamangar, S.; et al. The Influence of Reinforcement Particles Friction Stir Processing on Microstructure, Mechanical Properties, Tribological and Corrosion Behaviors: A Review. *J. Mater. Res. Technol.* **2022**, *20*, 1940–1975. [CrossRef]
5. Lee, T.; Jeong, W.; Chung, S.; Ryu, H.J. Effects of TiC on the Microstructure Refinement and Mechanical Property Enhancement of Additive Manufactured Inconel 625/TiC Metal Matrix Composites Fabricated with Novel Core-Shell Composite Powder. *J. Mater. Sci. Technol.* **2023**, *164*, 13–26. [CrossRef]
6. Singh, K.; Khanna, V.; Singh, S.; Bansal, S.A.; Chaudhary, V.; Khosla, A. Paradigm of State-of-the-Art CNT Reinforced Copper Metal Matrix Composites: Processing, Characterizations, and Applications. *J. Mater. Res. Technol.* **2023**, *24*, 8572–8605. [CrossRef]
7. Barakat, W.S.; Habba, M.I.A.; Ibrahim, A.; Fathy, A.; Elkady, O.A. The Effect of Cu Coated Al_2O_3 Particle Content and Densification Methods on the Microstructure and Mechanical Properties of Al Matrix Composites. *J. Mater. Res. Technol.* **2023**, *24*, 6908–6922. [CrossRef]
8. Reddy, P.V.; Kumar, G.S.; Krishnudu, D.M.; Rao, H.R. Mechanical and Wear Performances of Aluminium-Based Metal Matrix Composites: A Review. *J. Bio- Tribo-Corros.* **2020**, *6*, 83. [CrossRef]
9. Kumar, S.; Singh, R.; Hashmi, M.S.J. Metal Matrix Composite: A Methodological Review. *Adv. Mater. Process. Technol.* **2020**, *6*, 13–24. [CrossRef]
10. Abebe Emiru, A.; Sinha, D.K.; Kumar, A.; Yadav, A. Fabrication and Characterization of Hybrid Aluminium (Al6061) Metal Matrix Composite Reinforced with SiC, B_4C and MoS_2 via Stir Casting. *Int. J. Met.* **2023**, *17*, 801–812. [CrossRef]
11. Bharathi, P.; Kumar, T.S. Mechanical Characteristics and Wear Behaviour of Al/SiC and Al/SiC/B_4C Hybrid Metal Matrix Composites Fabricated through Powder Metallurgy Route. *Silicon* **2023**, *15*, 4259–4275. [CrossRef]
12. Xing, D.; Xi, X.-Y.; Liang, C.-G.; Ma, P.-C.; Zheng, Q.; Li, H. Thermoelectric Performance of Basalt Fiber with Nanocomposite Sizing. *Colloids Surf. A Physicochem. Eng. Asp.* **2023**, *672*, 131761. [CrossRef]
13. Farid, W.; Bah, T.A.; Kong, C.; Yu, H. A Novel Way to Fabricate High Elastic Modulus and High Strength of TiC Reinforced Aluminum Matrix Composite. *Mater. Manuf. Process.* **2023**, *38*, 1785–1797. [CrossRef]
14. Rajkumar, S.E.; Palanikumar, K.; Pitchandi, K.; Latha, B. Subsurface Integrity Studies on the Drilling of Al/B_4C/Mica Hybrid Metal Matrix Composites. *Mater. Manuf. Process.* **2020**, *35*, 52–60. [CrossRef]
15. Ramadoss, N.; Pazhanivel, K.; Ganeshkumar, A.; Arivanandhan, M. Microstructural, Mechanical and Corrosion Behaviour of B_4C/BN-Reinforced Al7075 Matrix Hybrid Composites. *Int. J. Met.* **2023**, *17*, 499–514. [CrossRef]
16. Hiremath, A.; Murthy, A.A.; Pranavathmaja, S.V.; Jajodia, A.; Sreenath, R. Effect of End Chills, Reinforcement Content and Carburization on the Hardness of LM25-Borosilicate Glass Particulate Composite. *J. Mech. Eng. Sci.* **2018**, *12*, 4203–4215. [CrossRef]
17. Samal, P.; Tarai, H.; Meher, A.; Surekha, B.; Vundavilli, P.R. Effect of SiC and WC Reinforcements on Microstructural and Mechanical Characteristics of Copper Alloy-Based Metal Matrix Composites Using Stir Casting Route. *Appl. Sci.* **2023**, *13*, 1754. [CrossRef]
18. Arya, R.K.; Kumar, R.; Telang, A. Influence of Microstructure on Tribological Behaviors of Al6061 Metal Matrix Composite Reinforced with Silicon Nitride (Si3N4) and Silicon Carbide (SiC) Micro Particles. *Silicon* **2023**, *15*, 3987–4001. [CrossRef]
19. Kumaresan, G.; Kumar, B.A. Investigations on Mechanical and Wear Properties of Al Matrix Composites Reinforced with Hybrid SiC and Al_2O_3 Micro-Particles. *Int. J. Met.* **2023**, *17*, 980–987. [CrossRef]
20. Karthikraja, M.; Ramanathan, K.; Loganathan, K.T.; Selvaraj, S. Corrosion Behaviour of SiC and Al_2O_3 Reinforced Al 7075 Hybrid Aluminium Matrix Composites by Weight Loss and Electrochemical Methods. *J. Indian Chem. Soc.* **2023**, *100*, 101002. [CrossRef]

21. Ferraris, M.; Gili, F.; Lizarralde, X.; Igartua, A.; Mendoza, G.; Blugan, G.; Gorjan, L.; Casalegno, V. SiC Particle Reinforced Al Matrix Composites Brazed on Aluminum Body for Lightweight Wear Resistant Brakes. *Ceram. Int.* **2022**, *48*, 10941–10951. [CrossRef]
22. Xu, T.; Mei, Q.S.; Liao, L.Y.; Ma, Y.; Chen, Z.H.; Wang, Y.C.; Li, J.Y. A Comparative Study on the Microstructure and Strengthening Behaviors of Al Matrix Composites Containing Micro-and Nano-Sized B_4C Particles. *Mater. Sci. Eng. A* **2023**, *874*, 145066. [CrossRef]
23. Messer, O.; Ratzker, B.; Shilo, J.T.; Kalabukhov, S.; Sokol, M. The Effect of Coarse and Fine Ti_3SiC_2 Particle Reinforcement in Aluminum Matrix Composites. *J. Alloys Compd.* **2024**, *976*, 173150. [CrossRef]
24. Nayak, K.C.; Deshmukh, P.R.; Pandey, A.K.; Vemula, P.; Date, P.P. Microstructural, Physical and Mechanical Characterization of Grinding Sludge Based Aluminium Metal Matrix Composite. *Mater. Sci. Eng. A* **2020**, *773*, 138895. [CrossRef]
25. Omoniyi, P.; Adekunle, A.; Ibitoye, S.; Olorunpomi, O.; Abolusoro, O. Mechanical and Microstructural Evaluation of Aluminium Matrix Composite Reinforced with Wood Particles. *J. King Saud Univ. Sci.* **2022**, *34*, 445–450. [CrossRef]
26. Mohan, D.; Chinnasamy, B.; Naganathan, S.K.; Nagaraj, N.; Jule, L.; Badassa, B.; Ramaswamy, K.; Kathirvel, P.; Murali, G.; Vatin, N.I. Experimental Investigation and Comparative Analysis of Aluminium Hybrid Metal Matrix Composites Reinforced with Silicon Nitride, Eggshell and Magnesium. *Materials* **2022**, *15*, 6098. [CrossRef]
27. Malaki, M.; Tehrani, A.F.; Niroumand, B.; Abdullah, A. Ultrasonically Stir Cast SiO_2/A356 Metal Matrix Nanocomposites. *Metals* **2021**, *11*, 2004. [CrossRef]
28. Tirfe, D.; Woldeyohannes, A.; Hunde, B.; Batu, T.; Geleta, E. Investigating Mechanical and Physical Properties of Stir Casted Al6061/Nano Al_2O_3/Quartz Hybrid Composite. *Adv. Mech. Mater. Eng.* **2023**, *40*, 189–201. [CrossRef]
29. Matti, S.; Shivakumar, B.P.; Nagaral, M.; Shashidhar, S.; Siddappa, P.N.; Auradi, V. Mechanical and Tribological Behavior of Flyash, Red Mud and Mica Particles Reinforced Al7075 Alloy Hybrid Metal Composites. *Manuf. Rev.* **2022**, *9*, 11. [CrossRef]
30. Soundararajan, R.; Sathishkumar, A.; Kalaiarasan, K. *Evolution of A356 with Flyash Composites on Metallurgical Mechanical and Tribological Behaviour under Dry and Wet Conditions*; SAE Technical Paper; SAE: Pittsburgh, PA, USA, 2021.
31. Reddy, S.P.; Danda, J.M.R.; Kolli, M.; Yaramala, A. Artificial Neural Network Modelling of Aluminium/Al_2O_3/Fly Ash Hybrid Composites Prepared by Powder Metallurgy. *Int. J. Interact. Des. Manuf.* **2023**, 1–9. [CrossRef]
32. Sharma, S.K.; Saxena, K.K.; Kumar, N. Effect of SiC on Mechanical Properties of Al-Based Metal Matrix Composites Produced by Stir Casting. *Met. Sci. Heat Treat.* **2022**, *64*, 316–320. [CrossRef]
33. Ibrahim, T.K.; Yawas, D.S.; Dan-Asabe, B.; Adebisi, A.A. Taguchi Optimization and Modelling of Stir Casting Process Parameters on the Percentage Elongation of Aluminium, Pumice and Carbonated Coal Composite. *Sci. Rep.* **2023**, *13*, 2915. [CrossRef]
34. Saini, P.; Singh, P.K. Physical, Morphological, and Mechanical Characterization of Al-4032/GMP Composite Fabricated through Stir Casting. *JOM* **2022**, *74*, 1340–1349. [CrossRef]
35. Venkatesh, V.S.S.; Rao, G.P.; Patnaik, L.; Gupta, N.; Kumar, S.; Saxena, K.K.; Sunil, B.D.Y.; Eldin, S.M.; Al-kafaji, F.H.K. Processing and Evaluation of Nano SiC Reinforced Aluminium Composite Synthesized through Ultrasonically Assisted Stir Casting Process. *J. Mater. Res. Technol.* **2023**, *24*, 7394–7408. [CrossRef]
36. Hiremath, A.; Bhat, R. Experimental Analysis of the Thermal Properties of Fused Quartz-Reinforced Al-6061alloy Matrix Composites Using RSM Approach. *J. Mech. Sci. Technol.* **2020**, *34*, 1091–1097. [CrossRef]
37. Li, M.; Guo, Q.; Chen, L.; Li, L.; Hou, H.; Zhao, Y. Microstructure and Properties of Graphene Nanoplatelets Reinforced AZ91D Matrix Composites Prepared by Electromagnetic Stirring Casting. *J. Mater. Res. Technol.* **2022**, *21*, 4138–4150. [CrossRef]
38. Hiremath, A. Strength of Chilled Aluminum Alloyborosilicate Glass-Flyash Hybrid Composites. *Int. J. Mech. Eng. Technol.* **2018**, *9*, 90–96.
39. Kumar, M.S.; Sathisha, N.; Jagannatha, N. Tribo Mechanical Study on Aluminium A356 Reinforced Metal Matrix Composites Casted with Copper Chill. *J. Bio- Tribo-Corros.* **2023**, *9*, 56. [CrossRef]
40. Kumar, M.S.; Sathisha, N.; Manjnatha, S.; Niranjana, S.J.; Tamam, N.; Khan, M.I. Fatigue Surface Analysis of AL A356 Alloy Reinforced Hematite Metal Matrix Composites. *Biomass Convers. Biorefinery* **2023**, 1–13. [CrossRef]
41. Vijay Kumar, S.L.; Sreenivas Rao, K.V.; Sandeep, G.M.; Udayashankar, S. Synthesis and Characterization of Al356-ZrO_2-SiC Hybrid Composites. *J. Inst. Eng. Ser. D* **2023**, 1–10. [CrossRef]
42. Ravitej, Y.P.; Mohan, C.B.; Ananthaprasad, M.G. Dry Sliding Friction and Wear Behavior of LM13/Zircon/Carbon (HMMCs): An Experimental, Statistical and Artificial Neural Network Approach. *Tribol. Ind.* **2022**, *44*, 374. [CrossRef]
43. Yadav, B.N.; Muchhala, D.; Singh, P.; Gupta, G.; Venkat, A.N.; Mondal, D.P. Compressive Deformation Behavior of Al--SiC--MWCNTs Hybrid Composite Foam through Factorial Design of Experiments. *Trans. Indian Inst. Met.* **2020**, *73*, 223–234. [CrossRef]
44. Gupta, R.; Nanda, T.; Pandey, O.P. Tribological Characteristics of LM13 Alloy Based Ilmenite-Boron Carbide Reinforced Hybrid Composites for Brake Drum Applications. *Wear* **2023**, *522*, 204851. [CrossRef]
45. Khan, M.M.; Dixit, G. Evaluation of Microstructure, Mechanical, Thermal and Erosive Wear Behavior of Aluminum-Based Composites. *Silicon* **2020**, *12*, 59–70. [CrossRef]
46. Pradeep Kumar, J.; Robinson Smart, D.S.; Manova, S.; Akinwande, A.; Saravana Kumar, M. Mechanical and Tribological Assessment of AA7075 Reinforced Si_3N_4/TaC/Ti Hybrid Metal Matrix Composites Processed through Stir Casting Process. *Adv. Mater. Process. Technol.* **2023**, 1–23. [CrossRef]

47. Ramaswamy, A.; Perumal, A.V. Multi-Objective Optimization of Drilling EDM Process Parameters of LM13 Al Alloy-10ZrB_2-5TiC Hybrid Composite Using RSM. *J. Braz. Soc. Mech. Sci. Eng.* **2020**, *42*, 432. [CrossRef]
48. Agarwal, B.D.; Broutman, L.J.; Agarwal, B.D.; Broutman, L.J. *Analysis and Performance of Fiber Composites*, 2nd ed.; John Wiley & Sons: Hoboken, NJ, USA, 1990.
49. Das, D.; Kayal, N. Properties and Performance of Cordierite-Bonded Porous Silicon Carbide Membrane Prepared Using Waste Fly Ash and Other Oxide Additives. *Bull. Mater. Sci.* **2023**, *46*, 169. [CrossRef]
50. Manikandan, R.; Arjunan, T. V Microstructure and Mechanical Characteristics of CDA--B_4C Hybrid Metal Matrix Composites. *Met. Mater. Int.* **2021**, *27*, 885–899. [CrossRef]
51. Palanivendhan, M.; Chandradass, J. Fabrication and Characterization of ADC-12 Hybrid Composites Utilizing Lemon Grass Ash and Boron Nitride through Stir-Squeeze Casting Method. *Mater. Res. Express* **2023**, *10*, 116509. [CrossRef]
52. Strzałkowska, E. Morphology, Chemical and Mineralogical Composition of Magnetic Fraction of Coal Fly Ash. *Int. J. Coal Geol.* **2021**, *240*, 103746. [CrossRef]
53. Sharma, J.; Polizos, G. Hollow Silica Particles: Recent Progress and Future Perspectives. *Nanomaterials* **2020**, *10*, 1599. [CrossRef] [PubMed]
54. Ogunrinola, I.; Akinyemi, M.; Aizebeokhai, A.; Sule, R.; Sanni, S.; Boyo, H.; Omeje, M.; Babalola, P. Silica and Kaolin Reinforced Aluminum Matrix Composite for Heat Storage. *Rev. Adv. Mater. Sci.* **2023**, *62*, 20220305. [CrossRef]
55. Sun, G.; Zhang, J.; Hao, B.; Li, X.; Yan, M.; Liu, K. Feasible Synthesis of Coal Fly Ash Based Porous Composites with Multiscale Pore Structure and Its Application in Congo Red Adsorption. *Chemosphere* **2022**, *298*, 134136. [CrossRef] [PubMed]
56. Miryuk, O.; Fediuk, R.; Amran, M. Porous Fly Ash/Aluminosilicate Microspheres-Based Composites Containing Lightweight Granules Using Liquid Glass as Binder. *Polymers* **2022**, *14*, 3461. [CrossRef]
57. Li, K.-Q.; Kang, Q.; Nie, J.-Y.; Huang, X.-W. Artificial Neural Network for Predicting the Thermal Conductivity of Soils Based on a Systematic Database. *Geothermics* **2022**, *103*, 102416. [CrossRef]